



Additive-Manufacturing of 3D Glass-Ceramics down to Nanoscale Resolution

Journal:	<i>Nanoscale Horizons</i>
Manuscript ID	NH-COM-09-2018-000293.R2
Article Type:	Communication
Date Submitted by the Author:	06-Dec-2018
Complete List of Authors:	<p>Gailevičius, Darius; Vilnius University, Laser research center; Femtika LTD, Padolskytė, Viktorija; Vilnius University, Laser research center Mikoliunaite, Lina; Vilnius University, Department of Physical Chemistry, Faculty of Chemistry and Geosciences Sakirzanovas, Simas; Vilnius University, Department of Physical Chemistry, Faculty of Chemistry and Geosciences Juodkasis, Saulius; Swinburne University of Technology, Centre for Micro-Photonics; the Victorian Node of the Australian National Fabrication Facility, Melbourne Centre for Nanofabrication Malinauskas, Mangirdas ; Vilnius University, Laser Research Center</p>

'Conceptual Insights' statement

We introduce a new 3D nanoscale optical printing modality for high-temperature glass-ceramic materials by combining the ultrafast 3D laser nanolithography with calcination. The new pathway to inorganic 3D structures with micro- and nano-scale resolutions can be made with a tailored final material composition. Ultrafast laser additive manufacturing allows production of initial 3D structures with ultra-small (hundreds-of-nm) feature dimensions out of a hybrid organic-inorganic resist SZ2080. Then, a post-fabrication heating (sintering) at different temperatures reaching up to 1500 °C in the air atmosphere facilitates decomposition of organic components resulting in a formation of a pure inorganic glass-ceramic hybrid. Calcination provides a route for the continuous size control and formation of new materials for free-form nano-/micro-objects. The application field includes tailored narrow-band IR emission sources, chemically resilient and high temperature optical elements for sensor applications in nuclear power plants, industrial, open space and defense fields where advanced nano-ceramic 3D structured materials are used.



Cite this: DOI: 10.1039/xxxxxxxxxx

Additive-Manufacturing of 3D Glass-Ceramics down to Nanoscale Resolution[†]

Darius Gailevičius,^{*a,b} Viktorija Padolskytė,^a Lina Mikoliūnaitė,^{c‡} Simas Šakirzanovas,^{*c‡} Saulius Juodkazis,^{*d,e‡} and Mangirdas Malinauskas^{*a}

Received Date

Accepted Date

DOI: 10.1039/xxxxxxxxxx

www.rsc.org/journalname

Fabrication of a true-3D inorganic ceramic with resolution down to nanoscale (~ 100 nm) using sol-gel resist precursor is demonstrated. The method has an unrestricted free-form capability, control of the fill-factor, and high fabrication throughput. A systematic study of the proposed approach based on ultrafast laser 3D lithography of organic-inorganic hybrid sol-gel resin followed by a heat treatment enabled formation of inorganic amorphous and crystalline composites guided by the composition of the initial resin. The achieved resolution of 100 nm was obtained for 3D patterns of complex free-form architectures. Fabrication throughput of 50×10^3 voxels/s is achieved; voxel - a single volume element recorded by a single pulse exposure. A post-exposure thermal treatment was used to form a ceramic phase which composition and structure were dependent on the temperature and duration of the heat treatment as revealed by Raman micro-spectroscopy. The X-ray diffraction (XRD) showed a gradual emergence of the crystalline phases at higher temperatures with a signature of cristobalite SiO_2 , a high-temperature polymorph. Also, a tetragonal ZrO_2 phase known for its high fracture strength was observed. This 3D nano-sintering technique is scalable from nanoscale to millimeter dimensions and opens a conceptually novel route for optical 3D nano-printing of various crystalline inorganic materials defined by an initial composition for diverse applications for microdevices designed to function in harsh physical and chemical environments and at high temperatures.

1 Introduction

We show that a popular hybrid organic-inorganic sol-gel resist SZ2080 can be converted into a material with entirely different properties obtained via polymer-to-ceramic transition guided by a high temperature sintering and oxidation. The silica and zirconia precursors present in the (sol-gel) resist at $\sim 43\%$ wt. fraction as an inorganic component will lead to emergence of silica and zirconia crystalline phases in the final sintered ceramic material. Importantly, a proportional downscaling of the 3D polymerized object takes place with significant volume change of 40-50% dependent on an annealing protocol without distortion of the size

proportions of the initial 3D design. The temperature-guided re-sizing and the composition change can be potentially tailored to form 3D free-form patterns of complexity which is not amenable by other micro-/nano-fabrication methods.

In this study, we explore a possibility to apply ultrafast 3D laser nanolithography¹ in conjunction with heat-treatment² to acquire ceramic 3D structures in micro- and nano-scale. Laser fabrication allows for production of initial 3D structures with relatively small (hundreds-of-nm) feature sizes out of hybrid organic-inorganic material SZ2080³ (Fig. 1). Then, a post-fabrication sintering at different temperatures up to 1500°C in the air atmosphere facilitates decomposition of organic part $\sim 57\%$ wt. and results in the glass-ceramic hybrid material. Resolution in the final 3D structure is superior to that of the as-fabricated structures. Both, filled volume as well as complex free-form 3D objects can be resized and their structural composition changed.

Ultrafast lasers are extending their applications towards advanced nanoscale processing of materials in additive, subtractive and combined approaches⁴⁻⁷. Recently, additive manufacturing of 3D micro-/nano-structures followed by heat-treatment protocols for down-scaling their dimensions while keeping their initial geometry was reported⁸⁻¹⁰, yet the attention was not paid to an

^a Laser Research Center at Vilnius University, Saulėtekio Ave. 10, Vilnius, LT-10223, Lithuania; E-mail: darius.gailevicius@ff.vu.lt; mangirdas.malinauskas@ff.vu.lt

^b Femtika Ltd., Saulėtekio Ave. 15, Vilnius, LT-10224, Lithuania

^c Faculty of Chemistry and Geosciences, Vilnius University, Naugarduko Str. 24, Vilnius, LT-03225, Lithuania E-mail: simas.sakirzanovas@chf.vu.lt

^d Swinburne University of Technology, John St., Hawthorn 3122 Vic, Australia; E-mail: sjuodkazis@swin.edu.au

^e Melbourne Centre for Nanofabrication, the Victorian Node of the Australian National Fabrication Facility, 151 Wellington Rd., Clayton 3168 Vic, Australia

[†] - the term Nanoscale is used with accordance to the current ISO/TS 80004-1:2015 defining it as the length range approximately from 1 nm to 100 nm, and synonymous with sub-100 nm scale.

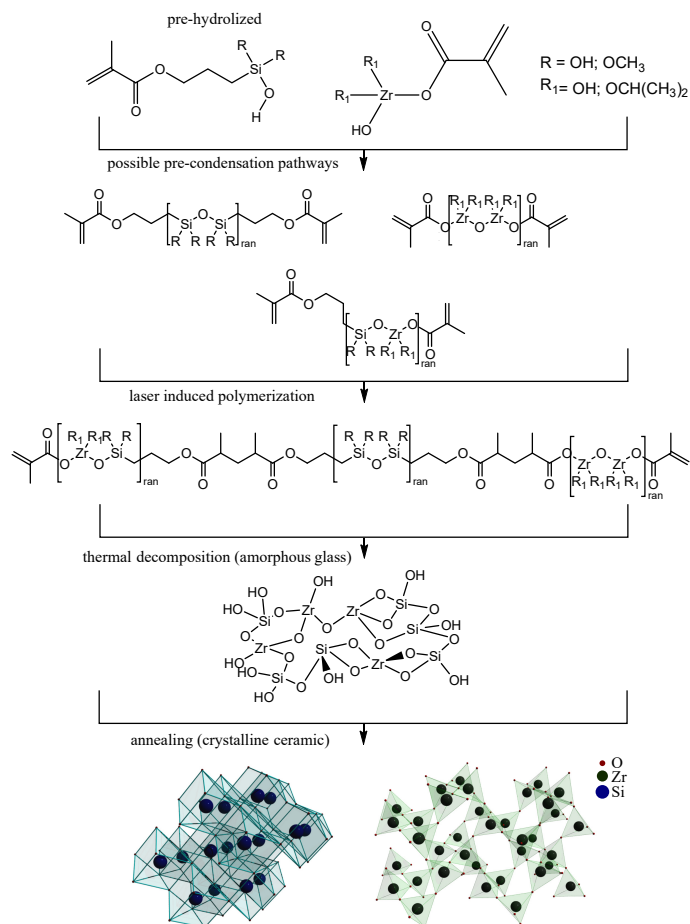


Fig. 1 Illustration of the main steps in synthesis of ceramics out of a hybrid SZ2080 sol-gel resist followed from laser induced polymerization that occurs during direct laser writing. Following the first stage of calcination, organic part is removed from the matrix and an inorganic glass matrix is formed. As temperature is increased further, crystallization occurs and polycrystalline ceramic phase forms. Crystal structure of cristobalite (left) and tetragonal zirconia ($t\text{-ZrO}_2$) (right) are shown in the bottom row.

experimentally validated explanation of material phase conversion processes¹¹, thus the potential advantages besides resizing were not investigated^{12,13}. Alternatively, the physical addition of metal nanoparticles resulted in a roughening of the structures after turning them fully into inorganic coatings¹⁴. This limits their applications for functional 3D nanostructures where pure inorganic materials and/or optical quality and structural uniformity of the patterns and workpieces are required¹⁵. Lastly, up to now there is no report on true-3D ceramic¹⁶ or glass^{17,18} structures with higher than tens-of-micrometers resolution despite specially designed pre-ceramic resins¹⁹.

Here, we show a straight-forward method to make 3D glass and ceramic structures with resolution down to the nanoscale with the final composition tailored by the initial materials.

2 Experimental

We used the widespread sol-gel prepolymer SZ2080 (IESL-FORTH, Greece) synthesized as described in³ for experiments

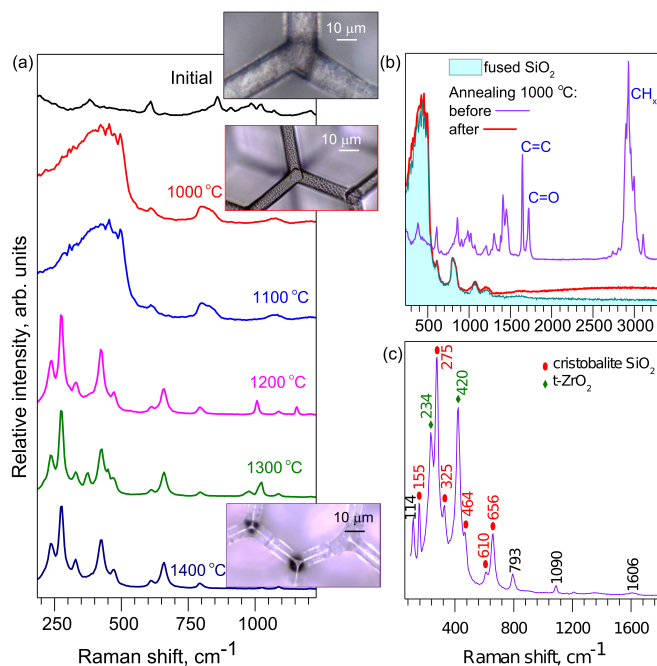


Fig. 2 Raman spectra of laser structured SZ2080 before and after heat-treatment (for 1 h in air). Disappearance of sharp peaks represents a changed make-up of the material after heat-treatment. (a) Change of Raman spectrum at several annealing temperatures; optical images of 3D-micro scaffolds ($T = 1000, 1400^\circ\text{C}$) from the sites where Raman spectra were measured. (b) Detailed spectrum of the initial structure and heat treated structure at $T = 1000^\circ\text{C}$ in comparison to the fused silica. (c) Raman spectrum after the highest temperature $T = 1400^\circ\text{C}$ annealing with peak matching to the cristobalite and tetragonal zirconia ($t\text{-ZrO}_2$).

of sintering/calcination. Photoinitiator was not used². 3D laser direct written structures were fabricated from this material and heat-treatment was performed in temperature range of 1000–1500°C. Changes in samples were analyzed by Raman spectroscopy and X-ray diffraction (XRD).

More specifically, for our experiment, we fabricated 3D structures with different geometries. These included all-volume polymerised cubes (bulk), 3D woodpile micro lattices (periodic), free form micro-sculptures which combined bulk volumes with nanoscale features of complex geometry, and macroscopic hexagonal 3D lattices which are usually used for cell scaffolds. Laser structuring was carried out with a ~ 300 fs duration, 515 nm wavelength, 200 kHz repetition rate pulses focused by objectives lenses of different numerical apertures NA from 0.8 to 1.4. Other relevant fabrication parameters were tuned to be approximately near the middle of the fabrication window²⁰, with one exception, where we produced a fine structure with a feature size of about ~ 140 nm. That required exposure at the bottom of the fabrication window²¹, which resulted into a lower cross-linking degree of the polymer matrix and increased shrinkage as well some geometrical deformation. Development of fabricated structures was carried out in methyl-isobutyl-ketone for one hour followed by treatment in a Piranha solution to remove organic contaminants from their surface. Fragile structures were dried in a super-critical CO_2 dryer to avoid mechanical changes due to capillary forces.

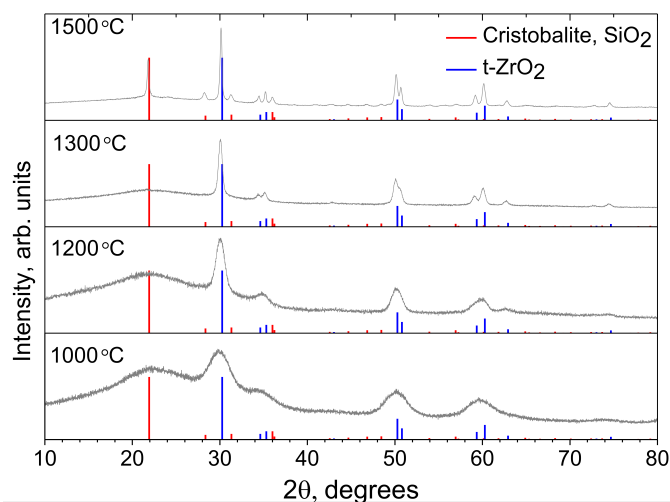


Fig. 3 X-ray diffraction (XRD) analysis of SZ2080 resist heat-treated at different temperatures for one hour in air at an ambient pressure. Broad peaks become more pronounced and evolve with temperature into sharp signature peaks of the two known crystalline phases of silica and zirconia.

The geometrical changes and fidelity of fabrication were tracked by optical and scanning electron microscopy (SEM).

For the (micro-)Raman spectral analysis we chose hexagonal scaffolds²², which are easy to handle as individual workpieces, due their millimeter scale. Micro-Raman spectra of the beams and intersections of the hexagonal scaffolds were measured at each relevant step: before and after heat treatment at different temperatures $T \leq 1500^\circ\text{C}$. To corroborate and interpret results we also performed an XRD analysis of the calcinated and then powdered SZ2080.

3 Results

The micro-Raman measurements are summarized in Fig. 2. As the temperature increases the spectral shape changes and evolves via qualitatively two distinct form-factors (Fig. 2). Close examination of the initial spectrum and comparison to that after annealing at $T = 1000^\circ\text{C}$ reveals that they differ by molecular vibrations which can be associated with the carbon-carbon, carbon-oxygen, carbon-hydrogen bonds. After heat-treatment those spectral lines vanishes (Fig. 2b). The new spectral form coincides with that typical for silica glass; spectra of a control sample of fused silica is shown.

Increasing the temperature further in steps of $\Delta T = 100^\circ\text{C}$ results in a new qualitative change of spectrum at $T = 1200^\circ\text{C}$. More pronounced peaks emerge with increased temperature. At the highest temperature (Fig. 2c), a few pronounced peaks become apparent. They coincide with vibrational signatures of the cristobalite²³ and tetragonal zirconia²⁴ (t-ZrO₂) phases, which are formed at high temperatures^{25,26}.

Figure 3 shows XRD data of annealed powder samples. At the lowest treatment temperature $T = 1000^\circ\text{C}$, broad peaks indicate formation of a glassy amorphous phase and only initial seeds of a crystalline phase. Also, the high background of XRD signal confirms a substantial amount of amorphous material. As

the temperature is increased, the peaks become exceedingly pronounced clearly showing an increasing dominance of the crystalline phase. The XRD peaks match well with reference data for cristobalite²⁷ and tetragonal zirconia²⁸, proving that annealed material is a mix of inorganic crystalline phases. From the XRD pattern, the period d which corresponds to the most pronounced peaks at the diffraction angle 2θ , given by the Bragg's condition $d = \lambda / (2 \sin \theta)$ can be estimated. The size L of the nano-crystalline phase follows from the Scherrer's equation $L = K\lambda / (B(2\theta) \cos \theta$; where $K = 0.89$ for spherical crystals and $B(2\theta)$ [rad] is the peak's angular bandwidth at full width half maximum. The Cu K α emission at $\lambda = 1.5406\text{\AA}$ was used. The most pronounced peaks are observed after treatment at $T = 1500^\circ\text{C}$ at Bragg diffraction angle $2\theta \approx 30.14^\circ$ and corresponds to the crystallite size of $L \approx 117.5$ nm for the t-ZrO₂ and similarly at the angle $2\theta \approx 21.82^\circ$ the size of cristobalite nano-crystallites was $L \approx 30.8$ nm. A size evolution of the t-ZrO₂ crystallites traced by the most prominent $\langle 111 \rangle$ XRD peak was $L \approx 1, 14, 118$ nm as temperature was increasing trough 1000, 1200, 1500°C, respectively.

As for the geometrical stability of the structures, they retain the same proportions up to $T \leq 1200^\circ\text{C}$, after which the structures show signs of melting and deformation. Sharp features become noticeably rounded by surface tension of the molten phase. We show that for the primary "glassy" phase, the structures retain their shape without distortion as shown in Fig. 4. The smallest geometrical features achieved are shown in Fig. 4(d) with an average cross section of a line 85 ± 10 nm measured at the middle point between the crossing junctions. True nanoscale (sub-100 nm dimensions) resolution can be achieved by the implemented processing. The effect of much higher temperatures is shown in the optical images in Fig. 2a.

4 Conclusions and Outlook

It is shown that by a high-temperature calcination of 3D polymerized structures, initially made by 3D laser writing in the organic-inorganic SZ2080, polymer resist produces either a silica-based glass or a polycrystalline ceramic pure inorganic material. Glass phase dominate in the samples annealed at moderate temperatures up to $\sim 1200^\circ\text{C}$. When samples are annealed above $\sim 1200^\circ\text{C}$ formation of polycrystalline silica and zirconia is observed, in particular, cristobalite and t-zirconia phases.

The presented modifications of silica-zirconia-rich resist SZ2080 from glass to polycrystalline ceramic by annealing shows a principle of the thermally guided 3D material printing which can reach true nanoscale (sub-100 nm) resolution. Isotropic down-sizing of the initial 3D polymerized objects with a volume fraction of 0.5-to-1 simplifies fabrication since there is no need to alter proportions of the initial material as it is widely used in DLW 3D nanolithography of photonic crystals, micro-optics and biomedical scaffolds in order to eliminate the effect of anisotropic shrinkage.

One can foresee a possibility to create required polymerizable mixtures which will lead to the final compounds of tailored composition - stoichiometry and size of polycrystalline phases according to the phase diagram^{29,30}. Mechanical and chemical properties of the final structures and objects will acquire new fea-

tures, especially resilience at harsh physical and chemical environments. Since nanoscale materials can initiate precipitation and guide growth of nano-crystallites, a wide field for experimentation horizons are widened by the presented modality of additive manufacturing.

One can foresee an alternative controlled calcination (or pyrolysis) method for a selected and partial modification of the initially polymerised structures which undergo thermal treatment. For example, focused electron or ion beam³¹ as well as a focused infrared laser radiation^{30,32} can be used to create required seed locations where new phases with novel properties will occur after annealing. This research avenue will be explored next.

Conflicts of interest

There are no conflicts to declare.

Acknowledgements

US AMRDEC grant No. W911NF-16-2-0069 "Enhanced Absorption in Stopped-Light Photonic Nanostructures: Applications to Efficient Sensing" project is acknowledged for the financial support. SJ is grateful for the partial support via ARC DP170100131 grant. Authors are thankful to Dr. M. Farsari group for providing SZ2080 material and sharing information of its composition.

Supplement

The supplement material contains the production protocol for SZ2080 powder and more detailed discussion of the changes to 3D direct laser written structures occurring at the ceramic state made via calcination route.

- Fig. S1. Large and magnified views of SEM micro-graphs of the Coat of arms sculpture.
- Fig. S2. SEM micro-graphs of 3D structures treated at 1200°C.
- Fig. S3. SEM micro-graphs of large-scale scaffold structure detailing the effects of heat-treatment at 1200°C.
- Fig. S4. Large-scale and close up views of SEM micro-graphs of the high-resolution woodpile 3D structures.

References

- 1 M. Malinauskas, A. Žukauskas, S. Hasegawa, Y. Hayasaki, V. Mizeikis, R. Buividas and S. Juodkazis, *Light Sci. Appl.*, 2016, **5**, e16133–e16133.
- 2 L. Jonusauskas, D. Gailevicius, L. Mikoliunaite, D. Sakalauskas, S. Sakirzanovas, S. Juodkazis and M. Malinauskas, *Materials*, 2017, **10**, 12.
- 3 A. Ovsianikov, J. Viertl, B. Chichkov, M. Oubaha, B. MacCraith, I. Sakellari, A. Giakoumaki, D. Gray, M. Vamvakaki, M. Farsari and C. Fotakis, *ACS Nano*, 2008, **2**, 2257–2262.
- 4 H. Wang, Y.-L. Zhang, H. Xia, Q.-D. Chen, K.-S. Lee and H.-B. Sun, *Nanoscale Horiz.*, 2016, **1**, 201–211.
- 5 Q.-K. Li, J.-J. Cao, Y.-H. Yu, L. Wang, Y.-L. Sun, Q.-D. Chen and H.-B. Sun, *Opt. Lett.*, 2017, **42**, 543–546.
- 6 X.-W. Cao, Q.-D. Chen, L. Zhang, Z.-N. Tian, Q.-K. Li, L. Wang, S. Juodkazis and H.-B. Sun, *Opt. Lett.*, 2018, **43**, 831–834.
- 7 H. Ding, Q. Zhang, Z. Gu and M. Gu, *Nanoscale Horiz.*, 2018, **3**, 312–316.
- 8 S. Passinger, M. Saifullah, C. Reinhardt, K. Subramanian, B. Chichkov and M. Welland, *Advanced Materials*, 2007, **19**, 1218–1221.
- 9 L. Guo, H. Xia, H.-T. Fan, Y.-L. Zhang, Q.-D. Chen, T. Zhang and H.-B. Sun, *Opt. Lett.*, 2010, **35**, 1695–1697.
- 10 G. Seniutinas, A. Weber, C. Padeste, I. Sakellari, M. Farsari and C. David, *Microelectron. Eng.*, 2018, **191**, 25–31.
- 11 J. Bauer, A. Schroer, R. Schwaiger and O. Kraft, *Nat. Mater.*, 2016, **15**, 438–443.
- 12 J. Li, B. Jia and M. Gu, *Opt. Express*, 2008, **16**, 20073–20080.
- 13 A. Zakhurdaeva, P.-I. Dietrich, H. Hölscher, C. Koos, J. G. Korvink and S. Sharma, *Micromachines*, 2017, **8**, 285.
- 14 A. Vyatskikh, S. Delalande, A. Kudo, X. Zhang, C. M. Portela and J. R. Greer, *Nat. Commun.*, 2018, **9**, 593.
- 15 T. Pham, D.-P. Kim, T.-W. Lim, S.-H. Park, D.-Y. Yang and K.-S. Lee, *Adv. Func. Mater.*, 2006, **16**, 1235–1241.
- 16 Z. C. Eckel, C. Zhou, J. H. Martin, A. J. Jacobsen, W. B. Carter and T. A. Schaedler, *Science*, 2015, **351**, 58–62.
- 17 F. Kotz, N. Schneider, A. Striegel, A. Wolfschläger, N. Keller, M. Worgull, W. Bauer, D. Schild, M. Milich, C. Greiner *et al.*, *Adv. Mater.*, 2018, **30**, 1707100.
- 18 F. Kotz, K. Arnold, W. Bauer, D. Schild, N. Keller, K. Sachsenheimer, T. Nargang, C. Richter, D. Helmer and B. Rapp, *Nature*, 2017, **544**, 337–339.
- 19 A. Zocca, C. M. Gomes, A. Staude, E. Bernardo, J. Günster and P. Colombo, *J. Mater. Research*, 2013, **28**, 2243–2252.
- 20 A. Žukauskas, I. Matulaitienė, D. Paipulas, G. Niaura, M. Malinauskas and R. Gadonas, *Laser Photon. Rev.*, 2018, **9**, 706–712.
- 21 V. Mizeikis, V. Purlys, R. Buividas and S. Juodkazis, *Journal of Laser Micro Nanoengineering*, 2014, **9**, 42.
- 22 J. Mačiulaitis, M. Deveikytė, S. Reikšytė, M. Bratchikov, A. Darinskas, A. Šimbelytė, G. Daunoras, A. Laurinavičienė, A. Laurinavičius, R. Gudas *et al.*, *Biofabrication*, 2015, **7**, 015015.
- 23 A. Ilieva, B. Mihailova, Z. Tsintsov and O. Petrov, *Amer. Mineralog.*, 2007, **92**, 1325–1333.
- 24 P. Barberis, T. Merle-Méjean and P. Quintard, *J. Nucl. Mater.*, 1997, **246**, 232–243.
- 25 A. Černok, K. Marquardt, R. Caracas, E. Bykova, G. Habler, H.-P. Liermann, M. Hanfland, M. Mezouar, E. Bobocioiu and L. Dubrovinsky, *Nat. Commun.*, 2017, **8**, 15647.
- 26 S. Vasanthavel, B. Derby and S. Kannan, *Dalton Trans.*, 2017, **46**, 6884–6893.
- 27 J. Pluth, J. Smith and J. Faber Jr, *J. Appl. Phys.*, 1985, **57**, 1045–1049.
- 28 P. Bouvier, E. Djurado, G. Lucazeau and T. Le Bihan, *Phys. Rev. B*, 2000, **62**, 8731.
- 29 C. Curtis and H. Sowman, *J. Amer. Ceram. Soc.*, 1953, **36**, 190–198.
- 30 R. Telle, F. Greffrath and R. Prieler, *Journal of the European Ceramic Society*, 2015, **35**, 3995–4004.
- 31 S. C. Das, A. Majumdar, S. Katiyal, T. Shripathi and R. Hippler, *Review of Scientific Instruments*, 2014, **85**, 025107.
- 32 S. Calixto, M. Rosete-Aguilar, F. J. Sanchez-Marin and L. C. neda Escobar, *Appl. Opt.*, 2005, **44**, 4547–4556.

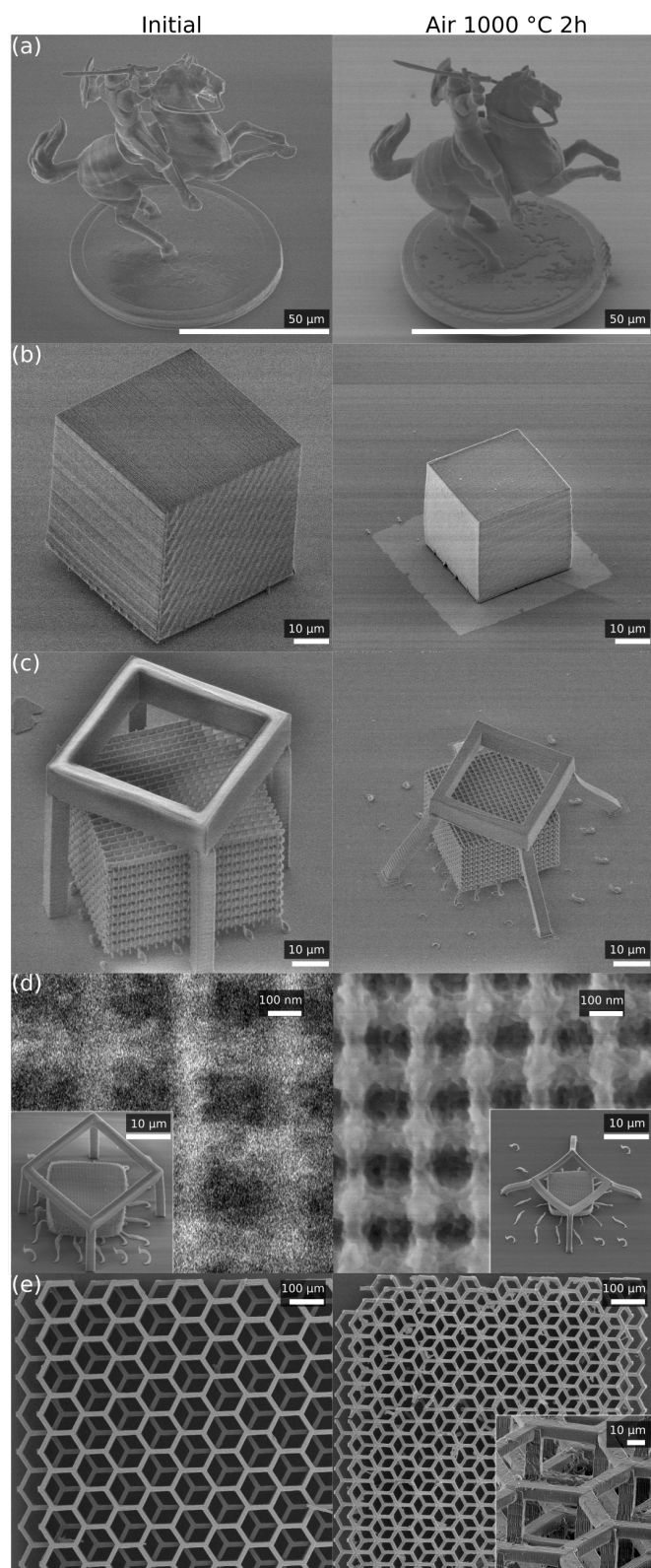


Fig. 4 Micro-graphs of different initial and treated structures (1000 °C for 2 h). Down-sizing of solid volumetric and free-form structures with correspondingly high and low initial volume fractions of polymer. From top to bottom: (a) a free-form sculpture of *Vytis* (Coat of arms of Lithuania), (b) homogeneous cube structure, (c) large and a (d) super-fine-featured photonic crystal structure with cage, and (e) hexagonal scaffold.